

# Experimental confirmation of Weber electrodynamics against Maxwell electrodynamics

Steffen Kühn  
steffen.kuehn@quantino-theory.de

April 22, 2019

This article examines by means of an easily reproducible experiment whether Maxwell electrodynamics or the almost forgotten Weber electrodynamics of Carl Friedrich Gauss and Wilhelm Weber is correct. For this purpose, it is shown that when charging a capacitor with two very flat and horizontally aligned plates a force on a permanent magnet should arise between the plates which differs in both theories diametrically in its direction. Subsequently, the measurement setup is described and, based on the measurement results, it is determined that Maxwell electrodynamics contradicts the experiment. The result of the experiment suggests that all aspects of modern physics should be subjected to a relentless and critical review.

## Contents

<b>1</b>	<b>Introduction</b>	<b>2</b>
<b>2</b>	<b>Basics</b>	<b>3</b>
2.1	The force between two uniformly moving point charges . . . . .	3
2.1.1	Weber force . . . . .	3
2.1.2	Maxwell force . . . . .	3
2.2	Forces between current elements . . . . .	5
2.3	Magnetic forces in a wire gap . . . . .	5
2.4	Solution of Maxwell's equations for a wire stub . . . . .	10
<b>3</b>	<b>Experiment</b>	<b>13</b>
3.1	Experimental setup . . . . .	13
3.2	Measurement results and evaluation . . . . .	15

## 1 Introduction

Maxwell's equations have been very successful in describing electromagnetic waves for more than one hundred years. Their rise to the sole theory of electromagnetism begins with an article by James Clerk Maxwell in 1865 [Maxwell, 1865]. In this article he shows that from the complete set of Maxwell's equations, including the displacement current, a wave equation can be derived in which electromagnetic disturbances of the field propagate at the speed of light. His assumption was that light would be an electrical phenomenon. In 1886 Heinrich Hertz succeeded in experimentally generating and detecting electromagnetic waves for the first time [Hertz, 1887].

Due to the success of Maxwell's equations, Weber's electrodynamics, which was widespread at this time, was increasingly forgotten because it was not compatible with the invariance of electric charge. Today it is largely unknown, although there have always been a few scientists who have studied it ([O'Rahilly, 1965], [Assis, 1994], [Anonymous, 2018]). The reason for this is to be found in the fact that Weber's force allows a fundamentally different view of modern physics. Especially their symmetry and the possibility to explain Magnetism as an electrorelativistic multi-particle effect is fascinating. In addition, it seems to be possible to interpret gravity as an electrorelativistic effect of fourth order ([Assis, 1992], [Kühn, 2019]). Moreover, Weber's force provides a new way of interpreting quantum mechanics, since it makes it possible to explain the quantum mechanical double-slit experiment on the basis of ponderomotoric forces [Kühn, 2019].

The majority of all scientists probably firmly assume that Maxwell's equations are correct and without alternative due to their age. But that is actually no reason to take them for granted without verification. Even old theories should be questioned again and again, especially when they are illogical. Anyway, the author of this article has been suspecting for several years that Maxwell electrodynamics cannot be correct because it leads to strange predictions. For example, in Maxwell electrodynamics – in contrast to Weber electrodynamics – energy conservation, conservation of momentum and conservation of angular momentum are only fulfilled if the emitted electromagnetic waves are included. However, this also applies to the quasi-stationary case, and this leads repeatedly one or another to try to develop magnetic perpetual mobiles or reactionless drives. The existence of such machines can be doubted.

Such and similar plausibility considerations have finally convinced the author of this article that it is time to look for a viable, easy to follow and direct way to clarify once and for all which of the two electrodynamics is correct. The theory behind such an experiment, as well as the experiment itself, are described in this article. The result clearly shows that Maxwell electrodynamics provides false predictions even under everyday conditions.

## 2 Basics

### 2.1 The force between two uniformly moving point charges according to Maxwell and Weber

The following is about the electromagnetic force that a uniformly moving point charge  $q_s$  exerts onto another uniformly moving point charge  $q_d$ . The configuration is shown in figure 1. An approximation that neglects the magnetic component is the Coulomb law.

#### 2.1.1 Weber force

An extension of the Coulomb law, which also contains the magnetic part, is from Wilhelm Weber in 1846 [Weber, 1893]:

$$\vec{F}_W = \left(1 - \frac{\dot{r}^2}{2c^2} + \frac{r\ddot{r}}{c^2}\right) \frac{q_s q_d}{4\pi\epsilon_0} \frac{\vec{r}}{r^3}. \quad (1)$$

In this,  $\dot{r}$  is the radial velocity and  $\ddot{r}$  the radial acceleration.

Because of  $\dot{\vec{v}} := \dot{\vec{r}} = \vec{v}_d - \vec{v}_s$  and  $\ddot{\vec{r}} = \dot{\vec{v}}_d - \dot{\vec{v}}_s = 0$ , and by using the relations

$$\dot{r} = \frac{d}{dt} \sqrt{\vec{r} \cdot \vec{r}} = \frac{\vec{r} \cdot \dot{\vec{r}}}{r} = \frac{\vec{r} \cdot \vec{v}}{r} \quad (2)$$

and

$$\ddot{r} = \frac{d^2}{dt^2} \sqrt{\vec{r} \cdot \vec{r}} = \frac{\vec{r} \cdot \ddot{\vec{r}}}{r} - \frac{(\dot{\vec{r}} \cdot \dot{\vec{r}})^2}{r^3} + \frac{\dot{\vec{r}} \cdot \dot{\vec{r}}}{r} = -\frac{(\vec{r} \cdot \vec{v})^2}{r^3} + \frac{v^2}{r}. \quad (3)$$

the formula

$$\vec{F}_W(\vec{r}, \vec{v}) = \left(1 + \frac{v^2}{c^2} - \frac{3}{2} \left(\frac{\vec{r} \cdot \vec{v}}{r c}\right)^2\right) \frac{q_s q_d}{4\pi\epsilon_0} \frac{\vec{r}}{r^3} \quad (4)$$

follows. Equation (4) is referred to in the following as **Weber force**.

#### 2.1.2 Maxwell force

Also from Maxwell's equations a formula can be derived which gives the electromagnetic force between two uniformly moving point charges. To get to this, it is necessary to solve

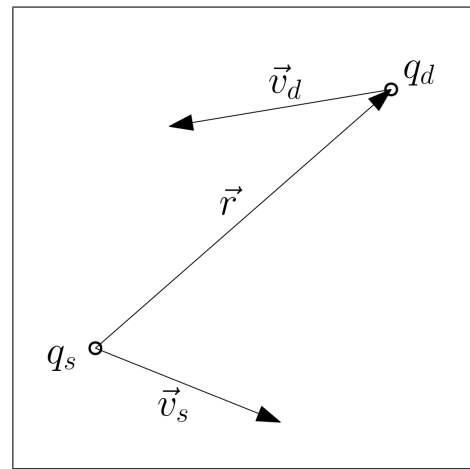


Figure 1: Configuration

Maxwell's equations. For point charges, the special solution is called Liénard-Wiechert potentials [Lehner, 2004, page 618].

If the point charge  $q_s$  is at the coordinate origin at the time  $t = 0$  and moves uniformly away from there with the velocity  $\vec{v}_s$  the scalar potential is

$$\varphi = \frac{c q_s}{4 \pi \varepsilon_0 \sqrt{(c^2 t - \vec{v}_s \vec{r})^2 + (c^2 - v_s^2) (r^2 - c^2 t^2)}}, \quad (5)$$

while the vector potential  $\vec{A}$  is

$$\vec{A} = \frac{\vec{v}_s}{c^2} \varphi. \quad (6)$$

By using the equations [Lehner, 2004, page 451]

$$\vec{E} = -\nabla \varphi - \frac{\partial \vec{A}}{\partial t} \quad (7)$$

and

$$\vec{B} = \nabla \times \vec{A}. \quad (8)$$

it is possible to obtain the electric field strength

$$\vec{E} = \frac{c q_s (c^2 - v_s^2) (\vec{r} - \vec{v}_s t)}{4 \pi \varepsilon_0 \sqrt{(r^2 - c^2 t^2) (c^2 - v_s^2) + (c^2 t - \vec{r} \vec{v}_s)^2}^3} \quad (9)$$

and the magnetic flux density

$$\vec{B} = \frac{\vec{v}_s}{c^2} \times \vec{E}. \quad (10)$$

Without loss of generality the time can be set to  $t = 0$  in equation (9) and it follows

$$\vec{E} = \frac{c q_s (c^2 - v_s^2) \vec{r}}{4 \pi \varepsilon_0 \sqrt{r^2 (c^2 - v_s^2) + (\vec{r} \vec{v}_s)^2}^3}. \quad (11)$$

The formula (10) remains unaffected by this.

However, the fields  $\vec{E}$  and  $\vec{B}$  themselves are not actually measurable, but only their force effects on test charges. In order to calculate the force  $\vec{F}$  onto another point charge  $q_d$ , additionally its velocity  $\vec{v}_d$  and the formula of the Lorentz force  $\vec{F} = q_d \vec{E} + q_d \vec{v}_d \times \vec{B}$  is needed. By inserting the equations (11) and (8) follows the relation

$$\vec{F}_M(\vec{r}, \vec{v}_s) = \frac{c (c^2 - v_s^2)}{\sqrt{(c^2 - v_s^2) + \left(\frac{\vec{r}}{r} \vec{v}_s\right)^2}^3} \frac{q_s q_d}{4 \pi \varepsilon_0 r^3} \left( \vec{r} + \frac{1}{c^2} \vec{r} \times \vec{v}_s \times \vec{v}_d \right) \quad (12)$$

for the force of one uniformly moving ideal point charge  $q_s$  onto another uniformly moving ideal point charge  $q_d$ . The equation (12) is referred to in the following as **Maxwell force**.

Both formulas – the Weber force (4) and the Maxwell force (12) – differ fundamentally. At least one of the formulas must be wrong.

## 2.2 Forces between current elements

Measuring the electromagnetic force directly between two moving point charges is practically impossible. Much easier is to measure the force between currents. For this reason, this section analyzes two oppositely equal charges  $q_s$  and  $-q_s$ , which are at the coordinate origin at the time  $t = 0$  and are moving at the speed  $\vec{v}_s/2$  and  $-\vec{v}_s/2$ .

It is obvious that the both oppositely moving charges will no longer be in the same place after only a short time. However, if one imagines many such current elements arranged in a line, it becomes clear that there are always two oppositely equally sized charges at one location at any given time, since the neighbors repeatedly replace the outflowing charge carriers. Such a line represents a direct current, because electric current is defined as the number of charge carriers passing through a surface transverse to the direction of movement per unit of time.

The force  $\vec{F}_{WC}$  of such a current element on a charge  $q_d$  with the velocity  $\vec{v}_d$  at the location  $\vec{r}$  is, when using the Weber force (4),

$$\begin{aligned}\vec{F}_{WC} &= \vec{F}_W(\vec{r}, \vec{v}_d - \vec{v}_s/2) - \vec{F}_W(\vec{r}, \vec{v}_d + \vec{v}_s/2) \\ &= \left( 3 \left( \frac{\vec{r}}{r} \vec{v}_s \right) \left( \frac{\vec{r}}{r} \vec{v}_d \right) - 2 \vec{v}_s \vec{v}_d \right) \frac{q_s q_d}{4 \pi \varepsilon_0 c^2} \frac{\vec{r}}{r^3}.\end{aligned}\quad (13)$$

For the Maxwell force (12) follows

$$\begin{aligned}\vec{F}_{MC} &= \vec{F}_M(\vec{r}, -\vec{v}_s/2) - \vec{F}_M(\vec{r}, +\vec{v}_s/2) \\ &= \frac{c (c^2 - (v_s/2)^2)}{\sqrt{(c^2 - (v_s/2)^2) + \left( \frac{\vec{r}}{r} (\vec{v}_s/2) \right)^2}^3} \frac{q_s q_d}{4 \pi \varepsilon_0 c^2 r^3} \vec{r} \times \vec{v}_s \times \vec{v}_d \\ &= \frac{q_s q_d}{4 \pi \varepsilon_0 c^2 r^3} \vec{r} \times \vec{v}_s \times \vec{v}_d + \mathcal{O}(v_s^2).\end{aligned}\quad (14)$$

## 2.3 Magnetic forces in a wire gap

The magnetic force of a current element on a moving point charge is given in Maxwell electrodynamics by the equation (14). In Weber electrodynamics, on the other hand, the equation (13) applies. Nevertheless, despite these two different formulas, the force between two closed conductive loops of any shape and at any distance is identical [Assis, 1990]. A decision between Maxwell and Weber electrodynamics is therefore not possible on basis of force measurement between closed conductor loops. However, the predicted forces differ if the wires are not closed. This is shown and discussed at this section.

The force of a current element on another current element is the sum of the force of the current element on a positive point charge  $q_d$  at the location  $\vec{r}$  with the velocity  $\vec{v}_d/2$  and the force on an inversely equal point charge at the same location with the opposite

velocity. In Maxwell's electrodynamics, the force of a current element on a point charge is given by the equation (14). The force of one current element onto another current element is therefore because of  $q_d \vec{v}_d/2 + (-q_d)(-\vec{v}_d/2) = q_d \vec{v}_d$  and  $1/\mu_0 = c^2 \epsilon_0$ ,

$$\vec{F}_M(\vec{r}) = \frac{\mu_0 q_s q_d}{4 \pi r^3} \vec{r} \times \vec{v}_s \times \vec{v}_d. \quad (15)$$

In Weber electrodynamics this force is given by the equation (13) and it applies

$$\vec{F}_W(\vec{r}) = \frac{\mu_0 q_s q_d}{4 \pi r^3} \left( 3 \left( \frac{\vec{r}}{r} \cdot \vec{v}_s \right) \left( \frac{\vec{r}}{r} \cdot \vec{v}_d \right) - 2 \vec{v}_s \cdot \vec{v}_d \right). \quad (16)$$

To get the force that an entire wire exerts onto a current element, the line integral along the wire has to be calculated.

Now two forces shall be calculated, namely

- the force of a wire which is located on the x-axis, begins at  $-\infty$  and ends at the coordinate origin and
- the force of a wire which is located on the x-axis, begins at the coordinate origin and ends at  $+\infty$ .

Of course, no permanent current flow is possible in such wire segments, since the current flow changes the total charge over time. On short time scales, however, the current is sufficiently uniform so that the configuration can be considered quasi-stationary.

With  $q_s \rightarrow \lambda_s$  and  $I_s = \lambda_s v_s \vec{e}_x$  for the Maxwell electrodynamics follows

$$\begin{aligned} \vec{F}_{IM}^{(\pm)}(\vec{r}, \vec{v}_d) &= \int_0^{\infty} \vec{F}_M(\vec{r} \pm s \vec{e}_x) ds \\ &= \frac{\mu_0 I_s q_d}{4 \pi r} \frac{\vec{r} \times \vec{e}_x \times \vec{v}_d}{(r \pm x)}. \end{aligned} \quad (17)$$

For Weber electrodynamics, on the other hand, the result is

$$\begin{aligned} \vec{F}_{IW}^{(\pm)}(\vec{r}, \vec{v}_d) &= \int_0^{\infty} \vec{F}_W(\vec{r} \pm s \vec{e}_x) ds \\ &= \vec{F}_{IM}^{(\pm)}(\vec{r}, \vec{v}_d) \pm \frac{\mu_0 I_s q_d (\vec{r} \cdot \vec{v}_d) \vec{r}}{4 \pi r^3}, \end{aligned} \quad (18)$$

which is the same result as in Maxwell's electrodynamics plus an additional term. The plus sign is valid for the wire to the left of the y-z plane and the minus sign for the wire to the right.

The figure 2 shows the fields of this force onto right hand directed current elements for a wire stub that is just positively charging. At the top the field is shown which follows from Maxwell electrodynamics. Below, the corresponding field is shown, which is predicted by Weber electrodynamics. It can be noticed, that – as was to be expected – currents which flow in the same direction attract each other.

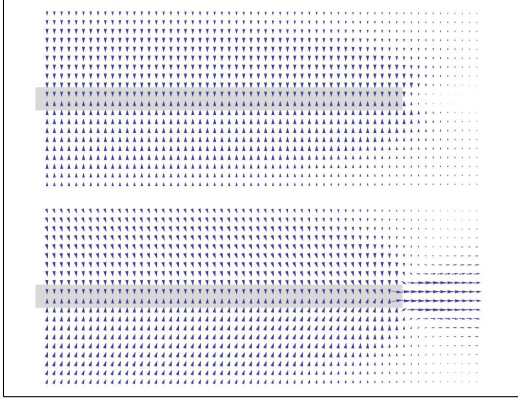


Figure 2:

not only be determined by integration, but also by solving the Maxwell equations directly. In section 2.4 this calculation is performed and it is shown that it is not absolutely necessary to use the Liénard-Wiechert potentials.

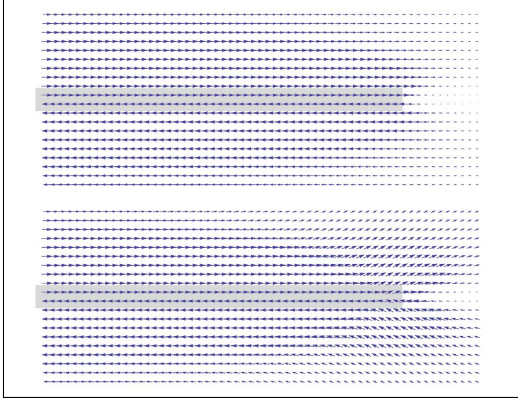


Figure 3:

ular unit vectors for which the equation

$$\vec{e}_a \times \vec{e}_b = \vec{\mu}/\mu \quad (19)$$

applies. For the total force  $\vec{F}_L$  on a conductor loop with the radius  $R$ , as one can see from the sketch 4, follows the equation

$$\vec{F}_L = R \int_0^{2\pi} \vec{F}_I \left( \vec{r} + R \vec{e}_\phi(\phi), \frac{I_d}{\lambda_d} \vec{e}_\phi(\phi + \pi/2) \right) d\phi \quad (20)$$

In figure 3 the fields for current elements with flow direction upwards are shown. The figures 2 and 3 show that the fields become more and more similar to each other on the left. This is also the reason why it is so difficult to distinguish between Maxwell and Weber electrodynamics simply by measuring the forces around direct currents. Only where the wire ends the fields differ. It is obvious that exactly this must be exploited in order to decide experimentally between the two theories.

It should be noted that for Maxwell's electrodynamics, the field of a wire stub cannot

But back to the experiment: The formulas (17) and (18) represent the force which the wire stub asserts onto current elements. For experiments, however, it is much more interesting to know which force and which torque acts on a small permanent magnet, since such a magnet is not influenced by an electric charge. Both will be calculated in the following. For this purpose it is assumed that at  $\vec{r}$  a very small conductor loop with the magnetic dipole moment  $\vec{\mu}$  is located (equivalent to a small permanent magnet). The figure 4 shows the configuration in form of a sketch.

Let  $\vec{e}_a$  and  $\vec{e}_b$  be two mutually perpendicular

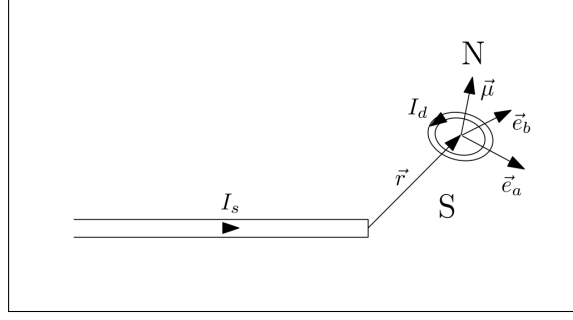


Figure 4:

with  $q_d \rightarrow \lambda_d$ ,

$$\vec{e}_\phi(\phi) := \vec{e}_a \cos(\phi) + \vec{e}_b \sin(\phi) \quad (21)$$

and

$$\mu = I_d \pi R^2. \quad (22)$$

For the torque  $\vec{M}_L$  follows quite equivalent according to the sketch the curve integral A1

$$\vec{M}_L = R^2 \int_0^{2\pi} \vec{e}_\phi(\phi) \times \vec{F}_I \left( \vec{r} + R \vec{e}_\phi(\phi), \frac{I_d}{\lambda_d} \vec{e}_\phi(\phi + \pi/2) \right) d\phi. \quad (23)$$

In order to solve the complicated integrals for the forces (17) and (18) it is useful to take advantage of the fact that the radius  $R$  of the conductor loop is very small, which allows a Taylor approximation of first order of  $\vec{F}_I$  at zero. The resulting approximation can then be used to obtain the force

$$\vec{F}_{LM}^{(\pm)}(\vec{r}) = \frac{\mu_0 I_s}{4\pi r^3} \left( \frac{r^2}{r \pm x} \vec{\mu} \times \vec{e}_x + \frac{(2r \pm x) \vec{r} \pm r^2 \vec{e}_x}{(r \pm x)^2} (\vec{\mu} \times \vec{r}) \cdot \vec{e}_x \right) \quad (24)$$

for Maxwell electrodynamics by using the equations (19) and (22). Weber electrodynamics, on the other hand, gives the force

$$\vec{F}_{LW}^{(\pm)}(\vec{r}) = \vec{F}_{LM}^{(\pm)}(\vec{r}) \pm \frac{\mu_0 I_s \vec{r} \times \vec{\mu}}{4\pi r^3}. \quad (25)$$

For the torque, Maxwell electrodynamics provides after calculation of the integral (23) and simplification of the terms the solution

$$\vec{M}_{LM}^{(\pm)}(\vec{r}) = \frac{\mu_0 I_s \vec{r} \times \vec{e}_x \times \vec{\mu}}{4\pi r (r \pm x)}. \quad (26)$$

For electrodynamics according to Weber follows

$$\vec{M}_{LW}^{(\pm)}(\vec{r}) = \vec{M}_{LM}^{(\pm)}(\vec{r}) \pm \frac{\mu_0 I_s \vec{r} \times \vec{\mu} \times \vec{r}}{4\pi r^3}. \quad (27)$$

The figures 5 and 6 show the total field of the two — slightly separated — wires on a permanent magnet with the north pole aligned into the drawing plane. Both wires together form a capacitor of low capacitance.

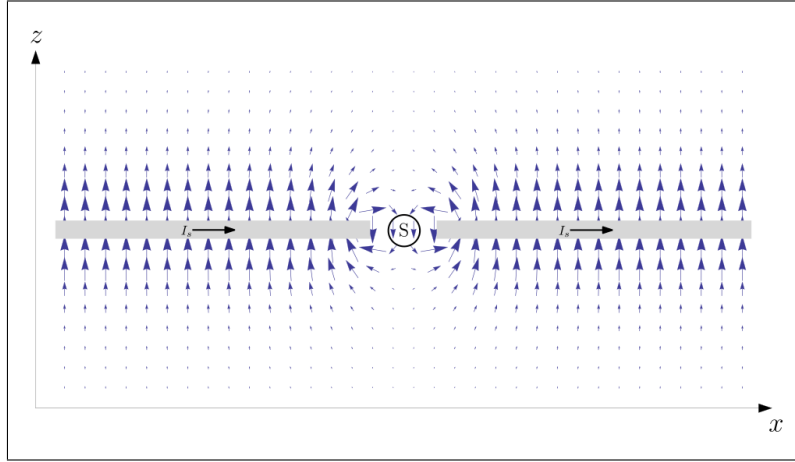


Figure 5: The force effect of a current according to Maxwell onto a permanent magnet with north pole pointing into the drawing plane.

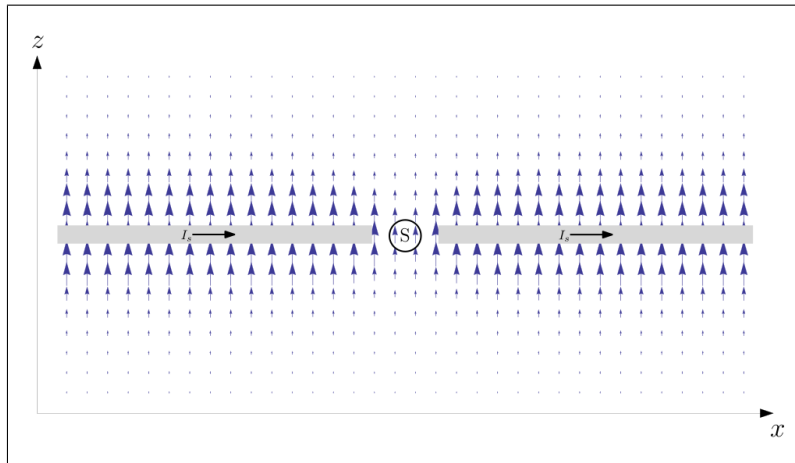


Figure 6: The force effect of a current according to Weber onto a permanent magnet with north pole pointing into the drawing plane.

Let  $d$  be the width of the air gap. The total force is then given by the equation

$$\vec{F}_T(\vec{r}) = \vec{F}_L^{(+)}(\vec{r} - d/2 \vec{e}_x) + \vec{F}_L^{(-)}(\vec{r} + d/2 \vec{e}_x). \quad (28)$$

It is obvious that in the middle of the wire gap forces occur that differ in sign. For Maxwell electrodynamics,  $\vec{\mu} = \mu \vec{e}_y$  (north pole points into the drawing plane) applies

$$\vec{F}_{TM}(\vec{0}) = -\frac{\mu_0 I_s \mu}{\pi d^2} \vec{e}_z, \quad (29)$$

while Weber electrodynamics predicts force

$$\vec{F}_{TW}(\vec{0}) = +\frac{\mu_0 I_s \mu}{\pi d^2} \vec{e}_z. \quad (30)$$

Both theories lead here to **opposite statements**, which makes a measurement of this force almost predestined for an experiment.

By the way, there is also something about torque that is worth mentioning. From equation (26) it is easy to deduce that  $\vec{M}_{LM}^{(\pm)}(\vec{r}) \cdot \vec{\mu} = 0$  applies, i.e. in Maxwell's electrodynamics is nowhere a torque which is aligned parallel to the magnetic moment  $\vec{\mu}$ . This is not the case in Weber electrodynamics! For example, when the magnet is positioned directly at the end of the wire stub. This is quite remarkable as it goes beyond the frame given by the magnetic field line concept. On the other hand, such a torque is necessary to ensure the conservation of the total angular momentum, since the magnet generates an angular momentum on the wire as well. A similar statement applies to the magnetic force in the air gap, since only in Weber electrodynamics the conservation of momentum is fulfilled.

## 2.4 Solution of Maxwell's equations for a wire stub

In this section, the field which was calculated in the previous section is determined again directly based on Maxwell's equations. This serves above all to show that the statement of Maxwell's electrodynamics regarding the previously calculated force effects does not depend on the solution path.

In this section the full set of Maxwell equations in vacuum is used:

$$\nabla \cdot \vec{E} = \frac{\rho}{\varepsilon_0} \quad (31)$$

$$\nabla \cdot \vec{B} = 0 \quad (32)$$

$$\nabla \times \vec{E} = -\frac{\partial \vec{B}}{\partial t} \quad (33)$$

$$\nabla \times \vec{B} = \mu_0 \vec{j} + \mu_0 \varepsilon_0 \frac{\partial \vec{E}}{\partial t}. \quad (34)$$

In the following, the electromagnetic field of a current-carrying wire is calculated, which lies exactly on the x-axis, begins somewhere far to the left and ends exactly at the coordinate origin. It is obvious that due to the current flow and the discontinuity, the wire cannot remain electrically neutral, but must charge or discharge over time. This

results in a time-varying electric field, which in turn must be taken into account in Ampère's circuital law (34).

As model for the current density of the wire stub the ansatz

$$\vec{j} = \frac{I_s}{2} \left( 1 - \operatorname{erf} \left( \frac{x}{\sqrt{2\nu}} \right) \right) g(y, \nu) g(z, \nu) \vec{e}_x \quad (35)$$

is used.  $I_s$  stands for the current and  $g$  for the Gaussian function:

$$g(u, \nu) := \frac{1}{\sqrt{2\pi\nu}} \exp \left( -\frac{u^2}{2\nu} \right). \quad (36)$$

The variance  $\nu$  can be very small for a real wire. In principle, an approach using distributions would also have been imaginable. However, the model (35) has the advantage that there are no singularities, which ensures that the fields are continuously differentiable everywhere. A transition to distributions can later be carried out after finding the solutions by calculating the limit  $\nu \rightarrow 0$ .

Inserting of equation (35) into the continuity equation

$$\frac{\partial \rho}{\partial t} + \nabla \cdot \vec{j} = 0 \quad (37)$$

yields the charge density

$$\rho = - \int \nabla \cdot \vec{j} dt = \frac{I_s t}{\sqrt{2\pi\nu}^3} e^{-\frac{r^2}{2\nu}} \quad (38)$$

with  $r^2 = x^2 + y^2 + z^2$ , assuming that the wire is electrically neutral at  $t = 0$ . The calculated charge density shows that the wire becomes electrically charged where it ends, since the current cannot flow on here.

To determine the electric field of this charge, the first Maxwell equation in integral form

$$\varepsilon_0 \oint_{\partial V} \vec{E} \cdot d\vec{A} = \iiint_V \rho dV \quad (39)$$

is used. The integral on the right corresponds to the charge  $Q$  enclosed in the volume. If a sphere with radius  $R$  is selected as volume than

$$Q = \int_0^{2\pi} \int_0^\pi \int_0^R \rho r^2 \sin(\theta) dr d\theta d\phi, \quad (40)$$

i.e.

$$Q = I_s t \left( \operatorname{erf} \left( \frac{R}{\sqrt{2\nu}} \right) - \sqrt{\frac{2}{\pi\nu}} R e^{-\frac{R^2}{2\nu}} \right). \quad (41)$$

Because of the spherical symmetry of the charge distribution  $\rho$ , it can be concluded that the electric field  $\vec{E}$  is also radially symmetric and that the field lines are always perpendicular to the surface of the sphere. The integral on the right side of the equation (39) can therefore be solved immediately and the result is

$$\varepsilon_0 \oint_{\partial V} \vec{E} \cdot d\vec{A} = \varepsilon_0 E 4 \pi R^2. \quad (42)$$

From the results (41) and (42) and the symmetry follows then

$$\vec{E} = \frac{I_s t \vec{r}}{4 \pi \varepsilon_0 r^3} \left( \operatorname{erf} \left( \frac{r}{\sqrt{2\nu}} \right) - \sqrt{\frac{2}{\pi\nu}} r e^{-\frac{r^2}{2\nu}} \right). \quad (43)$$

Next, the magnetic flux density  $\vec{B}$  can be determined by using the fourth of Maxwell's equations (34). For this purpose the current density (35) and the electric field (43) are used. Afterwards, Poincarés-Lemma can be applied and one gets to

$$\vec{B} = \frac{I_s \mu_0}{4 \pi (r^2 - x^2)} \left( 1 - \frac{x}{r} \operatorname{erf} \left( \frac{r}{\sqrt{2\nu}} \right) - e^{-\frac{r^2 - x^2}{2\nu}} \left( 1 - \operatorname{erf} \left( \frac{x}{\sqrt{2\nu}} \right) \right) \right) \vec{e}_x \times \vec{r}. \quad (44)$$

Inserting the equations (35), (43) and (44) in the four Maxwell equations (31) to (34) shows that all conditions are fulfilled. The equations (43) and (44) therefore describe the fields which, according to Maxwell's electrodynamics, result from the slow charging process of the wire stub.

Finally, the results can be simplified by calculating the limit  $\nu \rightarrow 0$ . For the current density follows

$$\vec{j} = I_s (1 - \Theta(x)) \delta(y) \delta(z) \vec{e}_x. \quad (45)$$

The electric field strength becomes

$$\vec{E} = \frac{I_s t \vec{r}}{4 \pi \varepsilon_0 r^3}, \quad (46)$$

and the magnetic flux density

$$\vec{B} = \frac{I_s \mu_0}{4 \pi (r^2 - x^2)} \left( 1 - \frac{x}{r} \right) \vec{e}_x \times \vec{r} = \frac{I_s \mu_0 \vec{e}_x \times \vec{r}}{4 \pi r (r + x)}. \quad (47)$$

Because of

$$\lim_{x \rightarrow -\infty} r(r + x) = \frac{1}{2}(y^2 + z^2) \quad (48)$$

and

$$\lim_{x \rightarrow -\infty} \vec{e}_x \times \vec{r} = \vec{e}_x \times \vec{r} \quad (49)$$

this magnetic field to the left of the  $y$ - $z$  plane changes into the usual field of a line current. On the right, however, the strength of the field decreases with the square of the distance to the  $y$ - $z$  plane, but otherwise retains its shape and orientation unchanged, just as if the current were still flowing slightly beyond the  $y$ - $z$  plane.

With the help of the Lorentz force

$$\vec{F} = q_d \vec{E} + q_d \vec{v}_d \times \vec{B}, \quad (50)$$

and by inserting the equations (46) and (47) one gets finally the force

$$\vec{F} = \frac{q_d I_s t \vec{r}}{4 \pi \varepsilon_0 r^3} + \frac{q_d I_s \mu_0 \vec{r} \times \vec{e}_x \times \vec{v}_d}{4 \pi r (r + x)}, \quad (51)$$

which the wire stub exerts on a point charge  $q_d$  with the velocity  $\vec{v}_d$  according to Maxwell's equations. A comparison shows that the magnetic part of the force corresponds exactly to formula (17).

## 3 Experiment

### 3.1 Experimental setup

In section 2.3 a way was identified to experimentally determine whether magnetostatics is correctly described by Maxwell's electrodynamics or by Webers approach. It was found that the simplest way is to measure the magnetic force on a permanent magnet within a wire gap. Both theories predict the same magnitude for the force, but the prediction differs diametrically in terms of direction. This predestines this effect for an experiment, since the direction of a force can be determined much more easily than its magnitude.

In figure 7 the basic experimental setup is shown. It consists of an upside-down U-shaped capacitor with an air gap. Exactly inside the gap is a rod-shaped permanent magnet hanging from a shielded piezoelectric cantilever force sensor (sensor: EKULIT EPZ-27MS44W, measuring method: [Virtanen u. a., 2018]). By closing a relay, the capacitor can be charged from 0 to 7kV via a series resistor. During this, a charging current flows for a short time in the plates and a displacement current within the wire gap. The permanent magnet, which is aligned with the north pole towards the observer, experiences during this charging event a magnetic force, which  $z$ -component can be measured as a voltage change of the piezoelectric sensor. The permanent magnet itself consists of 28 neodymium magnets with a diameter of 8mm and a total length of 86mm. To avoid dielectric breakdowns, the magnet was coated with an insulating coating.

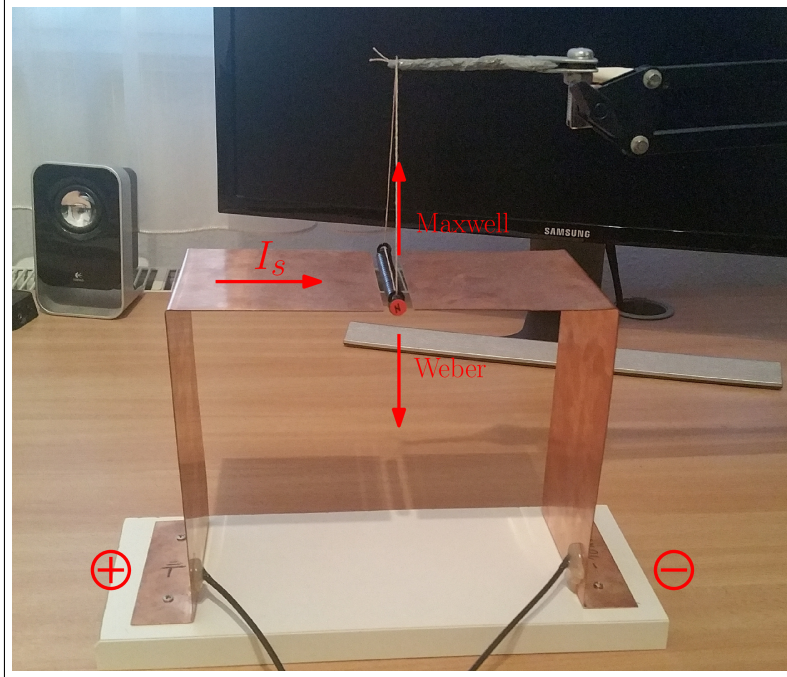


Figure 7: Experimental setup: measuring capacitor and permanent magnet with north pole directed towards the observer

As it becomes clear, the experiment is simple and direct. The only challenge is to reliably detect the small force that only acts for a short time. Furthermore, an electromagnetic pulse is generated during the charging event, which influences the measurement. Therefore, great importance must be attached to shielding. For this reason, the cantilever force sensor, on which the permanent magnet is suspended, was wrapped with electrically insulating foil and then with aluminium foil. The aluminium foil was then connected to the shield of a stereo audio cable in order to completely protect the two differential lines of the piezo up to the likewise shielded instrument amplifier. Figure 8 shows the remaining experimental setup consisting of charging circuit, trigger and measuring amplifier.

The schematic of the charging circuit is shown in figure 9. Here  $C_M$  is the measuring capacitor shown in figure 7. A measurement gave a capacity of about 8pF, of which only about one percent is due to the air gap. Since the high voltage source has a very large internal resistance  $R_i$ , there is a charging capacitor  $C_S$  parallel to the measuring capacitor, which ensures that the voltage of 7kV does not collapse when the relay  $S_1$  is closed and that there is enough charge available to charge the measuring capacitor.

As can be seen from the circuit, the measuring capacitor needs about  $2.4\mu s$  to be charged to 95 percent after closing the relay  $S_1$ , because the time constant  $\tau$  has the value  $R_C C_M = 0.8\mu s$ . This time constant specifies the pattern that can be expected from the piezo. The relay  $S_2$  and the resistor  $R_D$  are used to discharge the measuring capacitor

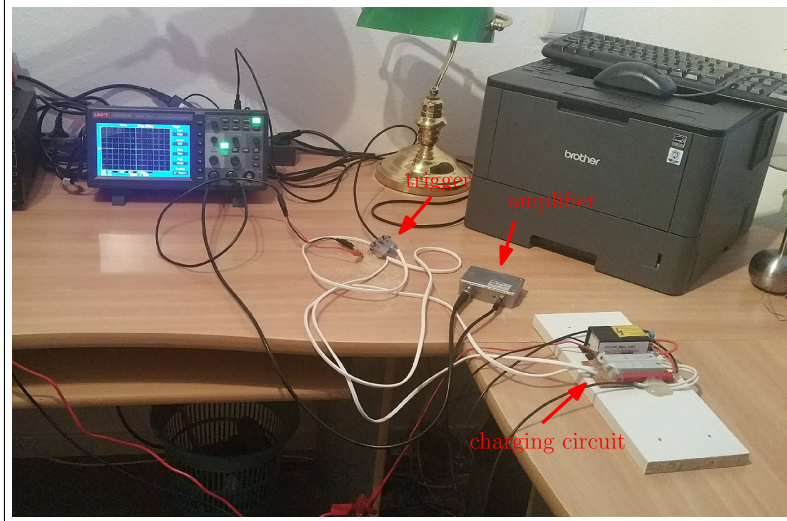


Figure 8: Experimental setup: charging circuit and measuring amplifier

and to establish a defined initial state.

Figure 10 shows the schematic of the amplifier. The INA111 is an integrated instrumentation amplifier, i.e. a differential amplifier with very high common mode rejection. Like the measuring cable to the sensor, the amplifier was completely shielded by installation in a metal housing.

### 3.2 Measurement results and evaluation

The forces generated at the piezoelectric cantilever force sensor are comparatively small. The magnetic moment  $\mu$  of the used neodymium magnet can be roughly estimated to the value  $3.8\text{Am}^2$  with the help of the formula  $\mu \approx \text{volume} \cdot 875000\text{A/m}$ . With a gap width of 12mm and an initial charge current of 70mA, the formula (29) respectively (30) gives a force of at most  $\pm 738\mu\text{N}$ , which corresponds to the weight force acting on an object with a mass of 75mg. In reality, this force will be much smaller, since only a fraction of the current flowing into the measuring capacitor is effective as displacement current in the air gap.

Fortunately, in this experiment it is not necessary to measure the magnitude of the force, since only its direction is of interest. For this reason, it is sufficient to clearly identify the force effect and to distinguish it from existing interference influences. Figure 11 shows in (A) the measured voltages of six different individual measurements on the piezoelectric cantilever force sensor immediately after switching on the relay  $S_1$ , exactly for the case shown in Figure 7. The current flows here from left to right and the north pole points in the direction of the beholder. (B) shows the voltages measured when the current flows from right to left.

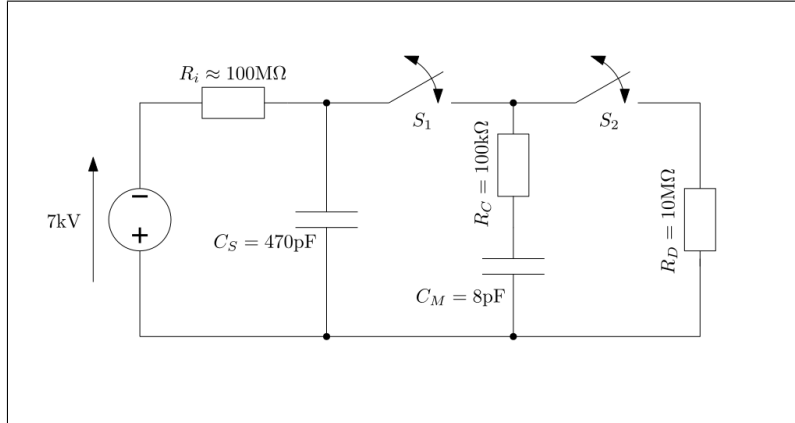


Figure 9: charging circuit

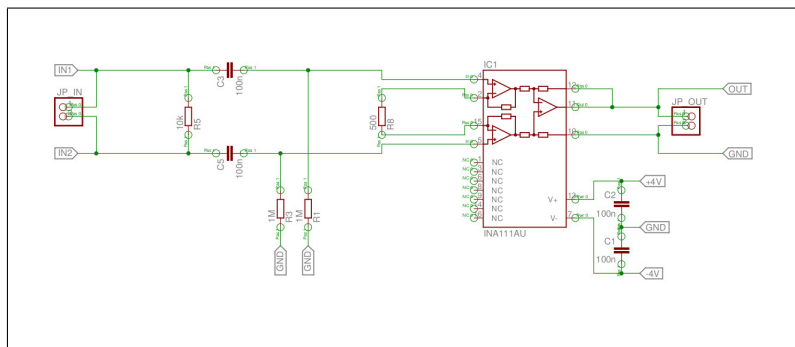


Figure 10: measuring amplifier

What is noticeable at first when looking at the figure 11 are the seemingly random peaks, where the first peak always occurs at about  $t = 14\mu\text{s}$ . The reason for this delay is that the relay needs some time between triggering and closing. The peak itself is an effect of the electromagnetic pulse in the oscilloscope itself and can be measured even when the magnet is disconnected from the force sensor or the amplifier is turned off. The peaks can therefore be regarded as disturbances. The voltage curves following a peak, however, are important for the experiment.

As can be seen, the voltage in figure 11 (A) approaches the x-axis after the first peak coming from below, while the opposite is true for (B). The shape of the voltage curve is thereby exponential, where the time constant is about  $2\mu\text{s}$ . This is in good agreement with the time constant previously derived from the circuit in Figure 9. It is therefore possible to conclude that the voltage curves observed are each due to the magnetic force, which is proportional to the charging current in the capacitor.

The randomly distributed peaks following the first peak show the significant pattern as well. The randomness of the occurrence can be explained by the bouncing of the relay,

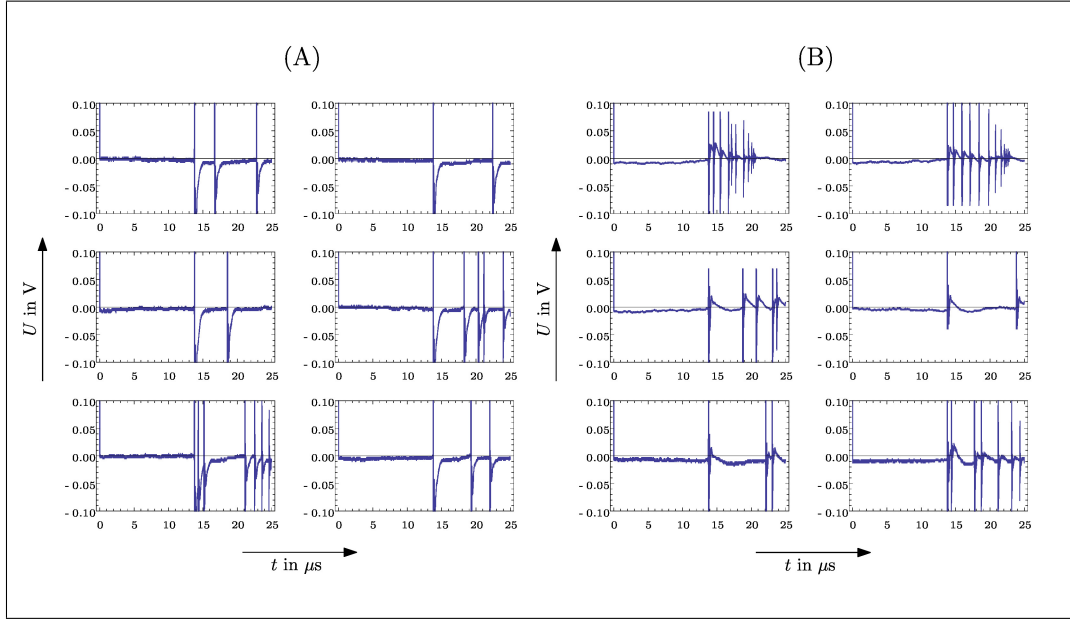


Figure 11: Measurement results: In (A) is Plus (Ground) on the left and Minus on the right. For (B) the capacitor is rotated, but the north pole is still pointing towards the beholder.

which opens and closes several times for a short time after triggering.

The bottom line is that if the current flows from left to right, the cantilever force sensor outputs a voltage change downwards, while if the current flows from right to left, the voltage rises. By tapping the force sensor very lightly, it could be determined that a voltage drop corresponds to a downward pulling force. A voltage rise, on the other hand, corresponds to a force that pushes from bottom to top.

This finally makes it evident that a charging current flowing from right to left results in a downward force, provided that the north pole of the magnet points in the direction of the beholder. However, a current flowing from right to left pushes the magnet upwards. This **corresponds to the predictions of Weber electrodynamics**, as can be seen in the figures 5 and 6, and shows at the same time that Maxwell electrodynamics is in contradiction with the experiment.

## 4 Summary and conclusion

This article showed that Weber and Maxwell electrodynamics can be experimentally distinguished by measuring the magnetic force directions within capacitors that are being charged or discharged. Subsequently, such an experiment was carried out and it was determined on the basis of the measurement results that the measured force direction

does not correspond to the predictions of Maxwell electrodynamics and that nature seems to follow Weber's law of force.

The consequences of this statement are extremely far-reaching and there are no words with which this can be sufficiently emphasized. If Maxwell's equations should be really wrong – and everything points to it – this would be the end of modern physics in its present form. The main problem is that virtually everything that was added to physics in the twentieth century is based on Maxwell's equations and is thus indirectly affected. Especially the Lorentz transformation has to be questioned, because it was created by Hendrik Antoon Lorentz only for the reason to explain the Maxwell equations. The magnetism of Weber's electrodynamics, on the other hand, is Galilean-invariant. For this reason, it can be assumed that particle physics, as well as astrophysics, are massively affected by subsequent errors, since both areas are based on relativistic dynamics.

Finally, the author feels compelled to make an urgent appeal to the entire scientific community and to demand that everything is questioned, regardless of the origin of a theory. Moreover, it has to be clarified how it was possible that such a fatal flaw remained undiscovered for so long.

## References

- [Anonymous 2018] ANONYMOUS: *Advances in Weber and Maxwell Electrodynamics*. Amazon Fulfillment, 2018
- [Assis 1990] ASSIS, André Koch T.: Deriving Ampere's Law from Weber's Law. In: *Hadronic Journal* 13 (1990), S. 441–451. – URL [https://www.ifi.unicamp.br/~assis/Hadronic-J-V13-p441-451\(1990\).pdf](https://www.ifi.unicamp.br/~assis/Hadronic-J-V13-p441-451(1990).pdf)
- [Assis 1992] ASSIS, André Koch T.: Deriving Gravitation from Electromagnetism. In: *Canadian Journal of Physics* (1992). – URL [https://www.ifi.unicamp.br/~assis/Can-J-Phys-V70-p330-340\(1992\).pdf](https://www.ifi.unicamp.br/~assis/Can-J-Phys-V70-p330-340(1992).pdf)
- [Assis 1994] ASSIS, André Koch T.: *Weber's electrodynamics*. Kluwer Acad. Publ., Dordrecht, 1994. – ISBN ISBN 0-7923-3137-0
- [Hertz 1887] HERTZ, Heinrich: Ueber sehr schnelle electrische Schwingungen. In: *Annalen der Physik* (1887), Nr. Band 267, Nummer 7. – URL [https://zs.thulb.uni-jena.de/servlets/MCRFileNodeServlet/jportal\\_derivate\\_00146629/18872670707 ftp.pdf](https://zs.thulb.uni-jena.de/servlets/MCRFileNodeServlet/jportal_derivate_00146629/18872670707 ftp.pdf)
- [Kühn 2019] KÜHN, Steffen: *Ein inhärent relativistischer Force-Carrier-Ansatz zur Vereinheitlichung von Elektromagnetismus und Gravitation auf Basis der Weber-Elektrodynamik*. 2019. – URL [www.quantino-theory.org](http://www.quantino-theory.org)
- [Lehner 2004] LEHNER, Günther: *Elektromagnetische Feldtheorie*. Springer-Verlag Berlin Heidelberg New York, 2004 (ISBN 3-540-00998-1)

- [Maxwell 1865] MAXWELL, James C.: A dynamical theory of the electromagnetic field. In: *Philosophical Transactions of the Royal Society of London* (1865). – URL <http://rstl.royalsocietypublishing.org/content/155/459>
- [O’Rahilly 1965] O’RAHILLY, A.: *Electromagnetic Theory: A Critical Examination of Fundamentals*. Dover Publications, 1965. – URL <http://archive.org/details/ElectrodynamicsORahilly>
- [Virtanen u. a. 2018] VIRTANEN, Juhani ; SARIOLA, V ; TUUKKANEN, Sampo: Piezoelectric cantilever force sensor sensitivity measurements. In: *Journal of Physics: Conference Series* 1065 (2018), 08, S. 042005. – URL [https://www.researchgate.net/publication/328893514\\_Piezoelectric\\_cantilever\\_force\\_sensor\\_sensitivity\\_measurements](https://www.researchgate.net/publication/328893514_Piezoelectric_cantilever_force_sensor_sensitivity_measurements)
- [Weber 1893] WEBER, Wilhelm E.: *Wilhelm Weber’s Werke (Band 3). Galvanismus und Elektrodynamik. Erster Teil*. Königliche Gesellschaft zu Göttingen, 1893. – URL <https://archive.org/stream/wilhelmweberswe02fiscgoog>